Space-Time-Range Adaptive Processing for MIMO Radar Imaging

Baoxin Chen, Yong Huang, Xiaolong Chen, Jian Guan
Naval Aviation University
Yantai, China
593691780@qq.com,

***Abstract*—Multiple-input multiple-output (MIMO) radar has drawn considerable attention due to its superior performance over phased array radar. The performance is achieved through waveform diversity. In terms of MIMO radar space-time adaptive processing (STAP), it is often assumed that the received signals has already been separated by a bank of matched filters (MFs) or the covariance matrix of the waveforms is an identity matrix. We find that when the non-complete orthogonality of the waveforms is taken into consideration, MIMO radar STAP suffers performance degradation. Besides, inspired by the definition of waveform diversity, a space-time-range adaptive processing (STRAP) scheme is proposed based on the framework of adaptive pulse compression (APC) and the criterion of minimum variance distortionless response (MVDR) to overcome the influence of non-completely orthogonal waveforms by taking into account the interference of nearby range cells to estimate the covariance matrix. The proposed algorithms are assessed via simulation experiments in two scenarios in comparison with sequential processing and the results show the effectiveness of STRAP.**

Keywords—MIMO radar; space-time-range adaptive processing; waveform separation; adaptive pulse compression

I. INTRODUCTION

In past few years, multiple-input multiple-output (MIMO) radar has gain great attention due to its advantages over phased array radar such as higher angle resolution, superior flexibility of transmit beampattern, stronger clutter and jam suppression capability, and better electromagnetic concealment [1-4]. The enhanced performance of MIMO radar depends on waveform diversity which is achieved by transmitting multiple uncorrelated or partially correlated waveforms. If the waveforms scattered back by a target can be observed from different angles, then spatial diversity is exploited to combat the target fluctuation and this radar system is often termed as distributed or statistical MIMO radar. Conversely, if the target echo is observed from the same direction i.e. that the spacing of the antenna array elements is comparable to the wavelength, thus the coherent signal processing or beamforming can be utilized and this kind of system is termed as coherent or collocated MIMO radar. In this paper, we focus on coherent MIMO radar imaging.

In MIMO radar, the received signals on each element is a superposition of the transmitted multiple waveforms with different Doppler frequency, from different directions and at different distances. Separating these waveforms effectively is basic to the realization of the above-mentioned merits. Generally, there are two ways to separate these waveforms: design a set of completely orthogonal waveforms or design a bank of excellent filters. The ideal orthogonal waveforms must satisfy that the cross-correlation of any two waveforms equals zero and the autocorrelation function has a very high peak sidelobe ratio. The literature about MIMO radar waveform design is emerging, but it is difficult to design such a set of coding waveforms within a finite waveform length and with a good Doppler tolerance. Moreover, the transmitted waveforms cannot be completely orthogonal in practice. In order to separate the waveform effectively, higher requirements are put forward for the pulse compression filter. A bank of matched filters (MFs) are often used to separate these non-completely orthogonal waveforms [5]. However, MFs suffer from range sidelobes and bad impact of the non-zero cross-correlation of the waveforms. Adaptive pulse compression (APC) is an effective method for mitigating the aforementioned problems, which adaptively estimates the filter weight for each individual range cell and waveform [6, 7]. In airborne MTI radar, space-time adaptive processing (STAP), which exploits the space domain and time domain jointly to suppress ground clutter, is a classic adaptive processing technique [8]. However, in MIMO radar STAP, it is often assumed that the transmitted waveforms are completely orthogonal i.e. that the covariance matrix is an identity matrix [9]. Nevertheless, it's impractical and we find that when the transmitted waveforms is not completely orthogonal, STAP suffers serious performance loss. Furthermore, the clutter and noise covariance matrix of the cell under test (CUT) is estimated with the Reed-Mallet-Brennan (RMB) criterion[10] by using the surrounding range cells which presumed to be target free and homogeneous i.e. that the training samples are independent and identically distributed (i.i.d.)[10]. Of course in practice, there is no guarantee of that, so the common methods such as Capon suffers performance loss. The iterative adaptive approach (IAA) for angle-Doppler imaging [11] following MFs or APC is an effective method for conventional phased-array radar, but for MIMO radar especially with non-completely orthogonal waveforms and nearby interference it works unsatisfactorily. IAA, which is the same as APC in nature, is first proposed in [12] for passive array processing and active sensing in single-antenna system. Then IAA is further employed in Range-Doppler imaging in [13]. In [14], IAA is extended to the application of MIMO

This work was supported in part by the National Natural Science Foundation of China (61471382, 61501487, U1633122, 61531020), the National Defense Technology Fund (2102024), the China Postdoctoral Science Foundation (2017M620862), and the Special Funds of Taishan Scholars of Shandong and Young Talents Program of CAST.

radar angle-Doppler-range imaging. However, the iterative process for the CUT using all the received samples, as in practice, the number of range cells is usually much larger than the length of the waveform, thus the computational burden is unbearable. Besides, as an extension to the APC in [6], space-range and time-range adaptive processing are proposed in [15] and [16] respectively and show enhanced performance over sequential processing. Consequently, it's natural to think of a joint space-time-range adaptive processing (STRAP, or joint angle-Doppler-range processing) for MIMO radar. Thus, based upon above analysis, the advantages of STRAP for MIMO radar can be summarized as follows:

1. Solve the problems that MFs cannot separate the waveforms effectively and APC-based cascaded processing suffers performance degradation in the multi-target condition.

2. Alleviate the requirements for a large number of i.i.d. training samples.

3. Better clutter suppression due to the increased degrees of freedom of the system.

The necessity of space-time-range adaptive processing is also approved by IEEE Standard Radar Definition 686-2008 [17, 18], in which waveform diversity is stated as follows:

Waveform Diversity: Optimization (possibly in a dynamically adaptive manner) of the radar waveform to maximize performance according to particular scenarios and tasks. May also jointly exploit other domains, including the antenna radiation pattern (both on transmit and receive), time domain, frequency domain, coding domain and polarization domain.

As can be seen from the definition, waveform diversity is a broad concept that involves a joint exploitation of multi-domain adaptive processing and it is also the remarkable feature of MIMO radar. We consider herein the STRAP to obtain a high resolution angle-Doppler-range imaging for MIMO radar. By taking into account the interference of nearby range cells to estimate the covariance matrix, two algorithms based on the framework of APC and the criterion of minimum variance distortionless response (MVDR) are developed and evaluated.

II. DISCRETE SIGNAL MODEL AND PROBLEM FORMULATION

Consider a MIMO uniform linear array (ULA) with N_{T} transmit antennas spaced at d_{T} and N_{R} receive antennas spaced at d_{R}. The transmit waveforms $\mathbf{S}=\left[\mathbf{s}_1 \quad \mathbf{s}_2 \quad \cdots \quad \mathbf{s}_{N_{\mathrm{T}}}\right]^{\mathrm{T}} \in \mathbb{C}^{N_{\mathrm{T}}\times N_{\mathrm{W}}}$ are narrowband, of which the nth row contains the length-N_{W} discretized waveform.

Assume that the intra-pulse Doppler shift can be neglected and multiple targets can exist within the same range-angle cell, then the mth pulse echo reflected from a solitary "point" scatterer with Doppler frequency f_{d}, angle θ, range cell l and complex scattering coefficient $\alpha(l,\theta,f_{\mathrm{d}})$ after down-conversion and analog-to-digital conversion can be written as

$$\mathbf{Y}(m,l,\theta,f_{\mathrm{d}})=\alpha(l,\theta,f_{\mathrm{d}})e^{j2\pi(m-1)f_{\mathrm{d}}T_{\mathrm{r}}}\mathbf{b}(\theta)\mathbf{a}^{\mathrm{T}}(\theta)\mathbf{S} \tag{1}$$

in which $(\bullet)^{\mathrm{T}}$ denotes the transpose operation, $\mathbf{a}(\theta)$ denotes the transmit array steering vector, $\mathbf{b}(\theta)$ is the receive array steering vector, and T_{r} is the pulse repetition interval (PRI). Vectorize (1) and stack N_{P} pulses of a coherent processing interval (CPI) in a vector form, we have

$$\begin{aligned}\mathbf{y}(l,\theta,f_{\mathrm{d}})&=\alpha(l,\theta,f_{\mathrm{d}})\mathbf{S}^{\mathrm{T}}\mathbf{a}(\theta)\otimes\mathbf{b}(\theta)\otimes\mathbf{u}(f_{\mathrm{d}})\\&\triangleq\alpha(l,\theta,f_{\mathrm{d}})\mathbf{V}(\theta,f_{\mathrm{d}})\end{aligned} \tag{2}$$

with $\otimes$ denoting the Kronecker product and $\mathbf{u}(f_{\mathrm{d}})$ being the temporal steering vector at Doppler frequency f_{d}. When there are other scatterers nearby the lth range cell, specifically at the $(l+p,\theta,f_{\mathrm{d}})$ range-angle-Doppler cell, the nearby interference can be modeled as

$$\begin{aligned}\mathbf{y}(l+p,\theta,f_{\mathrm{d}})&=\alpha(l+p,\theta,f_{\mathrm{d}})\left[\mathbf{J}^{\mathrm{T}}(p)\mathbf{S}^{\mathrm{T}}\mathbf{a}(\theta)\right]\otimes\mathbf{b}(\theta)\otimes\mathbf{u}(f_{\mathrm{d}})\\&\triangleq\alpha(l+p,\theta,f_{\mathrm{d}})\mathbf{V}(p,\theta,f_{\mathrm{d}})\end{aligned} \tag{3}$$

with $\mathbf{J}(p)\in\mathbb{C}^{N_{\mathrm{W}}\times N_{\mathrm{W}}}$ being the shift matrix defined by

$$\mathbf{J}_{i,j}(p)=\begin{cases}1, \text{if } i-j+p=0\\0, \text{if } i-j+p\neq 0\end{cases} \tag{4}$$

Taking all the nearby scatterers within $2P+1$ rang cells, N_{D} Doppler cells and N_{S} spatial cells into consideration, we can establish the discrete signal model as follow:

$$\mathbf{y}(l)=\sum_{\theta}\sum_{f_{\mathrm{d}}}\sum_{p=-P}^{P}\mathbf{y}(l+p,\theta,f_{\mathrm{d}})+\mathbf{n} \tag{5}$$

where $\mathbf{n}\in\mathbb{C}^{N_{\mathrm{P}}N_{\mathrm{R}}N_{\mathrm{W}}\times 1}$ is a circularly symmetric complex Gaussian random vector of additive noise samples with mean $\mathbf{0}$ and covariance matrix $\sigma^2\mathbf{I}$.

In terms of airborne MIMO radar, the system suffers performance degradation due to the ground clutter. Clutter is the interference related to the signal, which is spatially distributed in both azimuth and range and also spreads in Doppler domain due to the platform motion. The need for STAP in airborne MTI radar arises from the inherent relationship between the clutter azimuth and Doppler given by

$$f_{\mathrm{d,c}}=\beta\theta_{\mathrm{c}} \tag{6}$$

where β is a constant that depends on the platform speed, PRI and d_{R}. Then the clutter of the lth iso-range ring can be modeled as

$$\mathbf{y}_{\mathrm{c}}(l)=\sum_{\theta_{\mathrm{c}}}\sum_{p=-P}^{P}\mathbf{y}(l+p,\theta_{\mathrm{c}},\beta\theta_{\mathrm{c}}) \tag{7}$$

A bank of matched filters are used to separate these waveforms to form a virtual array. In order to keep the noise white after separation [5],

$$\mathbf{S}_{\mathrm{MF}}=\mathbf{S}^{\mathrm{H}}\left(\mathbf{S}\mathbf{S}^{\mathrm{H}}\right)^{-1/2} \tag{8}$$

is used as the matched filter bank with $(\bullet)^{\mathrm{H}}$ denoting the complex-conjugate transpose operation and $(\bullet)^{-1/2}$ denoting the inverse of the Hermitian square root of a matrix. Note that, in this paper we assume that the covariance matrix of the waveforms has full rank.

III. Space-Time-Rang Adaptive Processing

In traditional phased arrays, spatial beamforming is often followed by the MFs-based pulse compression, and then Doppler processing, detection or other processes. As for STAP, spatial beamforming and temporal (Doppler) processing are considered jointly to suppress clutter and indicate moving targets. For MIMO radar, extraction of the transmitted waveforms is often the first step, however, because of the non-complete orthogonality of transmitted waveforms, it is usually difficult for MFs to separate theses waveforms effectively. Hence the performance of the followed beamforming or Doppler processing is not satisfying. So in this section, a filter entitled MF-RMVDR is first proposed based on the outputs of MFs and then a STRAP filter is developed as a multi-dimensional extension of APC-RMMSE in [19]. This section is termed space-time-range adaptive processing, as both of the two algorithms can obtain an accurate angle-Doppler-range profile and the main difference is whether or not the processing is based on the outputs of MFs.

A. MF-RMVDR Filter

Here we consider an iterative adaptive processing to solve the problems that MFs cannot separate the waveforms effectively. The range-compressed signals for N_{R} receive elements and N_{P} pulses can be written as

$$\begin{aligned}\hat{\mathbf{y}}(l)&=\left(\mathbf{S}_{\mathrm{MF}}^{\mathrm{T}}\otimes\mathbf{I}_{N_{\mathrm{R}}}\otimes\mathbf{I}_{N_{\mathrm{P}}}\right)\mathbf{y}(l)\\&=\sum_{\theta}\sum_{f_{\mathrm{d}}}\sum_{p=-P}^{P}\alpha(l+p,\theta,f_{\mathrm{d}})\begin{bmatrix}\mathbf{S}_{\mathrm{MF}}^{\mathrm{T}}\mathbf{J}^{\mathrm{T}}(p)\mathbf{S}^{\mathrm{T}}\mathbf{a}(\theta)\\ \otimes\mathbf{b}(\theta)\otimes\mathbf{u}(f_{\mathrm{d}})\end{bmatrix}+\hat{\mathbf{n}}\\&\triangleq\sum_{\theta}\sum_{f_{\mathrm{d}}}\sum_{p=-P}^{P}\alpha(l+p,\theta,f_{\mathrm{d}})\hat{\mathbf{V}}(p,\theta,f_{\mathrm{d}})+\hat{\mathbf{n}}\end{aligned} \tag{9}$$

where $\hat{\mathbf{n}}=\left(\mathbf{S}_{\mathrm{MF}}^{\mathrm{T}}\otimes\mathbf{I}_{N_{\mathrm{R}}}\otimes\mathbf{I}_{N_{\mathrm{P}}}\right)\mathbf{n}$ is the filtered noise term which is still white. Using (9), we can obtain the output of transmit-receive-Doppler matched filter as

$$\hat{a}_{\mathrm{MF}}(l,\theta,f_{\mathrm{d}})=\frac{\hat{\mathbf{V}}^{\mathrm{H}}(\theta,f_{\mathrm{d}})\hat{\mathbf{y}}(l)}{\hat{\mathbf{V}}^{\mathrm{H}}(\theta,f_{\mathrm{d}})\hat{\mathbf{V}}(\theta,f_{\mathrm{d}})} \tag{10}$$

where $\hat{\mathbf{V}}(\theta,f_{\mathrm{d}})\triangleq\hat{\mathbf{V}}(0,\theta,f_{\mathrm{d}})$.

For MF-RMVDR filter, we use the following cost function to derive the optimum filter coefficient as

$$J(l,\theta,f_{\mathrm{d}})=\mathrm{E}\left[\left|\alpha(l,\theta,f_{\mathrm{d}})-\hat{\mathbf{w}}^{\mathrm{H}}(l,\theta,f_{\mathrm{d}})\hat{\mathbf{y}}(l)\right|^{2}\right] \tag{11}$$

where $\mathrm{E}(\bullet)$ is the expectation operator. Minimization of (11) with a unity gain constraint $\hat{\mathbf{w}}^{\mathrm{H}}(l,\theta,f_{\mathrm{d}})\hat{\mathbf{V}}(\theta,f_{\mathrm{d}})=1$ yields

$$\hat{\mathbf{w}}(l,\theta,f_{\mathrm{d}})=\left\{\mathrm{E}\left[\hat{\mathbf{y}}(l)\hat{\mathbf{y}}^{\mathrm{H}}(l)\right]\right\}^{-1}\begin{Bmatrix}\mathrm{E}\left[\alpha^{*}(l,\theta,f_{\mathrm{d}})\hat{\mathbf{y}}(l)\right]\\ -\dfrac{\lambda}{2}\hat{\mathbf{V}}(\theta,f_{\mathrm{d}})\end{Bmatrix} \tag{12}$$

in which $(\bullet)^{*}$ denotes the complex conjugate operation. Assuming the angle-Doppler-range cells are uncorrelated with each other as well as with the noise, we obtain

$$\hat{\mathbf{w}}(l,\theta,f_{\mathrm{d}})=\frac{\mathbf{R}^{-1}(l)\hat{\mathbf{V}}(\theta,f_{\mathrm{d}})}{\hat{\mathbf{V}}^{\mathrm{H}}(\theta,f_{\mathrm{d}})\mathbf{R}_{l}^{-1}\hat{\mathbf{V}}(\theta,f_{\mathrm{d}})} \tag{13}$$

where $\hat{\mathbf{R}}(l)=\sum_{\theta}\sum_{f}\sum_{p=-P}^{P}\hat{\mathbf{y}}(l+p,\theta,f_{\mathrm{d}})\hat{\mathbf{y}}^{\mathrm{H}}(l+p,\theta,f_{\mathrm{d}})+\hat{\mathbf{R}}_{\mathrm{NSE}}$ represents the total covariance matrix of the l iso-range ring with $\hat{\mathbf{R}}_{\mathrm{NSE}}$ denoting noise covariance matrix or the diagonal loading term. Any prior information regarding the noise can be used via $\hat{\mathbf{R}}_{\mathrm{NSE}}$. Note that (13) has the familiar form with MVDR, different from which the processing here is in a reiterative fashion, thus we call it MF-RMVDR filter.

B. STRAP Filter

Inspired by the above MF-RMVDR filter, in this section, we consider joint space-time-range adaptive processing directly. Different from the IAA in [14], the iterative process of STRAP filter uses only $2P+1$ range cells on both sides of the CUT, In fact, STRAP and MF-RMVDR can be regarded as a multi-dimensional extension of APC-RMMSE in [19] and MF-RMMSE in [20] respectively.

Similar to the derivation of MF-RMVDR, we can obtain the output of the space-time-range matched filter expressed as

$$\breve{\alpha}_{\mathrm{MF}}(l,\theta,f_{\mathrm{d}}) = \frac{\mathbf{V}^{\mathrm{H}}(\theta,f_{\mathrm{d}})\mathbf{y}(l)}{\mathbf{V}^{\mathrm{H}}(\theta,f_{\mathrm{d}})\mathbf{V}(\theta,f_{\mathrm{d}})} \tag{14}$$

and the STRAP filter as

$$\breve{\mathbf{w}}(l,\theta,f_{\mathrm{d}}) = \frac{\mathbf{R}^{-1}(l)\mathbf{V}(\theta,f_{\mathrm{d}})}{\mathbf{V}^{\mathrm{H}}(\theta,f_{\mathrm{d}})\mathbf{R}^{-1}(l)\mathbf{V}(\theta,f_{\mathrm{d}})} \tag{15}$$

where $\mathbf{R}(l) = \sum_{\theta}\sum_{f}\sum_{p=-P}^{P}\mathbf{y}(l+p,\theta,f_{\mathrm{d}})\mathbf{y}^{\mathrm{H}}(l+p,\theta,f_{\mathrm{d}}) + \mathbf{R}_{\mathrm{NSE}}$ is similar with the definition of the MF-RMVDR filter in (13).

IV. Implementation and Fast Matrix Update

A. Reiterative Processing

Since the covariance matrix $\hat{\mathbf{R}}(l)$ and $\mathbf{R}(l)$ are associated with the scattering coefficients of the surrounding cells which are usually unavailable in practice, thus a reiterative processing framework is utilized to estimate the angle-Doppler-range profile and the filter coefficients alternatively for both above algorithms. In order to speed up the implementation of the procedure, the three-in-one steering vectors $\mathbf{V}(p,\theta,f_{\mathrm{d}})$ and $\hat{\mathbf{V}}(p,\theta,f_{\mathrm{d}})$ can be calculated offline and stored. For MF-RMVDR, a bank of MFs are adopted to extract the transmitted waveforms to form a virtual array firstly, as shown in(9). Then the initial estimations of the angle-Doppler-range profile can be obtained by applying the matched filter outputs of (10) or (14), which are then used to construct the covariance matrix in (13) or (15). The new estimations can be obtained by using $\hat{\alpha}(l,\theta,f_{\mathrm{d}}) = \hat{\mathbf{w}}^{\mathrm{H}}(l,\theta,f_{\mathrm{d}})\hat{\mathbf{y}}(l)$ or $\breve{\alpha}(l,\theta,f_{\mathrm{d}}) = \breve{\mathbf{w}}^{\mathrm{H}}(l,\theta,f_{\mathrm{d}})\mathbf{y}(l)$. Repeat the above steps until the estimations of angle-Doppler-range profile converge or expected iterations are reached. Generally it converges within 5 iterations.

B. Fast Matrix Update

As the dimension of the covariance matrix $\hat{\mathbf{R}}(l)$ and $\mathbf{R}(l)$ are $N_{\mathrm{T}}N_{\mathrm{R}}N_{\mathrm{P}}$ and $N_{\mathrm{W}}N_{\mathrm{R}}N_{\mathrm{P}}$ respectively. A fast matrix update strategy based on the matrix inversion lemma can be used to alleviate the computational burden. We write $\mathbf{R}(l-1)$ in the following form:

$$\mathbf{R}(l-1) = \begin{bmatrix}\mathbf{B} & \mathbf{A}^{\mathrm{H}}\\ \mathbf{A} & \mathbf{C}\end{bmatrix} \tag{16}$$

where $\mathbf{A} \in \mathbb{C}^{(N_{\mathrm{P}}N_{\mathrm{R}}N_{\mathrm{W}}-N_{\mathrm{R}}N_{P})\times N_{\mathrm{R}}N_{P}}$ $\mathbf{B} \in \mathbb{C}^{N_{\mathrm{R}}N_{P}\times N_{\mathrm{R}}N_{P}}$ and $\mathbf{C} \in \mathbb{C}^{(N_{\mathrm{P}}N_{\mathrm{R}}N_{\mathrm{W}}-N_{\mathrm{R}}N_{P})\times(N_{\mathrm{P}}N_{\mathrm{R}}N_{\mathrm{W}}-N_{\mathrm{R}}N_{P})}$. For the next range cell, the covariance matrix can be written as

$$\mathbf{R}(l) = \begin{bmatrix}\mathbf{C} & \mathbf{D}\\ \mathbf{D}^{\mathrm{H}} & \mathbf{E}\end{bmatrix} \tag{17}$$

where $\mathbf{D} \in \mathbb{C}^{(N_{\mathrm{P}}N_{\mathrm{R}}N_{\mathrm{W}}-N_{\mathrm{R}}N_{P})\times N_{\mathrm{R}}N_{P}}$ and $\mathbf{E} \in \mathbb{C}^{N_{\mathrm{R}}N_{\mathrm{P}}\times N_{\mathrm{R}}N_{\mathrm{P}}}$. Thus we can write

$$\begin{aligned}\mathbf{R}(l) &= \mathbf{P}\mathbf{R}(l-1)\mathbf{P}^{\mathrm{T}} + \begin{bmatrix}\mathbf{D}-\mathbf{A} & \mathbf{0}\\ \mathbf{E}-\mathbf{B} & \mathbf{I}\end{bmatrix}\begin{bmatrix}\mathbf{0} & \mathbf{I}\\ \mathbf{D}^{\mathrm{H}}-\mathbf{A}^{\mathrm{H}} & \mathbf{0}\end{bmatrix}\\ &= \mathbf{Q}+\mathbf{U}\mathbf{V}\end{aligned} \tag{18}$$

where $\mathbf{P}$ is the permutation matrix and $\mathbf{P}^{-1} = \mathbf{P}^{\mathrm{T}}$. Using the matrix inversion lemma, we have

$$\mathbf{R}^{-1}(l) = \mathbf{Q}^{-1} - \mathbf{Q}^{-1}\mathbf{U}\left(\mathbf{I}+\mathbf{V}\mathbf{Q}^{-1}\mathbf{U}\right)^{-1}\mathbf{V}\mathbf{Q}^{-1} \tag{19}$$

in which $\mathbf{Q}^{-1} = \mathbf{P}\mathbf{R}^{-1}(l-1)\mathbf{P}^{\mathrm{T}}$, $\mathbf{U}$ and $\mathbf{V}$ are composed by the identity matrix $\mathbf{I}$ and

$$\begin{bmatrix}\mathbf{B}\\ \mathbf{A}\end{bmatrix} = \sum_{\theta}\sum_{f_{\mathrm{d}}}\sum_{p=-P}^{0}\begin{bmatrix}\left|\breve{\alpha}(l+p-1,\theta,f_{\mathrm{d}})\right|^{2}\tilde{s}_{-p}(\theta)\mathbf{J}^{\mathrm{T}}(p)\mathbf{S}^{\mathrm{T}}\mathbf{a}(\theta)\\ \otimes\left[\mathbf{b}(\theta)\mathbf{b}^{\mathrm{H}}(\theta)\right]\otimes\left[\mathbf{u}(f_{\mathrm{d}})\mathbf{u}^{\mathrm{H}}(f_{\mathrm{d}})\right]\end{bmatrix} \tag{20}$$

$$\begin{bmatrix}\mathbf{D}\\ \mathbf{E}\end{bmatrix} = \sum_{\theta}\sum_{f_{\mathrm{d}}}\sum_{p=0}^{P}\begin{bmatrix}\left|\breve{\alpha}(l+p,\theta,f_{\mathrm{d}})\right|^{2}\tilde{s}_{P-p-1}(\theta)\mathbf{J}^{\mathrm{T}}(p)\mathbf{S}^{\mathrm{T}}\mathbf{a}(\theta)\\ \otimes\left[\mathbf{b}(\theta)\mathbf{b}^{\mathrm{H}}(\theta)\right]\otimes\left[\mathbf{u}(f_{\mathrm{d}})\mathbf{u}^{\mathrm{H}}(f_{\mathrm{d}})\right]\end{bmatrix} \tag{21}$$

with $\tilde{s}_{p}$ being the pth entry of $\mathbf{S}^{\mathrm{T}}\mathbf{a}(\theta)$. Note that $\hat{\mathbf{V}}(\theta,f_{\mathrm{d}}) = \left(\mathbf{S}_{\mathrm{MF}}^{\mathrm{T}}\otimes\mathbf{I}_{N_{\mathrm{R}}}\otimes\mathbf{I}_{N_{\mathrm{P}}}\right)\mathbf{V}(p,\theta,f_{\mathrm{d}})$, thus for MF-RMVDR Filter, the covariance matrix $\hat{\mathbf{R}}(l)$ can be written as

$$\hat{\mathbf{R}}(l) = \left(\mathbf{S}_{\mathrm{MF}}^{\mathrm{T}}\otimes\mathbf{I}_{N_{\mathrm{R}}}\otimes\mathbf{I}_{N_{\mathrm{P}}}\right)\bar{\mathbf{R}}(l)\left(\mathbf{S}_{\mathrm{MF}}^{\mathrm{T}}\otimes\mathbf{I}_{N_{\mathrm{R}}}\otimes\mathbf{I}_{N_{\mathrm{P}}}\right)^{\mathrm{H}} \tag{22}$$

where $\bar{\mathbf{R}}(l)$ has the same structure as $\bar{\mathbf{R}}(l)$ in (18) and $\bar{\mathbf{R}}(l)$ is updated by the estimations of (10) or using(13). So the similar fast matrix update strategy for MF-RMVDR Filter can be obtained with minor adjustments. First, $\bar{\mathbf{R}}^{-1}(l)$ can be calculated by

$$\bar{\mathbf{R}}^{-1}(l-1) = \left(\mathbf{S}_{\mathrm{MF}}^{\mathrm{T}}\otimes\mathbf{I}_{N_{\mathrm{R}}}\otimes\mathbf{I}_{N_{\mathrm{P}}}\right)^{-1}\begin{bmatrix}\hat{\mathbf{R}}^{-1}(l-1)\\ \left(\mathbf{S}_{\mathrm{MF}}^{\mathrm{T}}\otimes\mathbf{I}_{N_{\mathrm{R}}}\otimes\mathbf{I}_{N_{\mathrm{P}}}\right)^{-\mathrm{H}}\end{bmatrix} \tag{23}$$

Then $\bar{\mathbf{R}}^{-1}(l)$ can be obtained by using the above update strategy for STRAP. Finally, $\hat{\mathbf{R}}^{-1}(l)$ is obtained by using (22).

V. Simulation Experiments and Results

This section uses simulation experiments to demonstrate the superior performance of the proposed algorithms over that of sequential processing such as sequential MF-IAA or sequential APC-IAA. Two different scenarios are assessed respectively. First an air surveillance scenario will be examined and then a MTI scenario with ground clutter is simulated according to (7). The MIMO radar under consideration has $N_T = 4$ transmitters spaced at $d_T = 2\lambda$ and $N_R = 4$ receivers spaced at $d_R = 0.5\lambda$ with λ being the wavelength. A set of polyphase coded waveforms in [21] with $N_W = 40$ are chosen to be the transmitted waveforms, which are designed with good correlation. The number of pulses in a CPI is $N_P = 8$ and the PRI $T_r = 0.0005$ s. We divide the lth iso-range ring of the illuminated scene into $N_S = N_D = 81$ spatial and Doppler cells and insert a total of 12 targets at the angle-Doppler-range map as described in Tab. 1. The noise power is set to be a constant -20 dB. Note that the angle and Doppler values in Tab. 1 are normalized. The range CUT are set to be 20 and has 4 targets with different angles and Doppler frequencies, as shown in Fig. 1(a). Target locations are denoted by white circles. The other 8 targets with relatively high SNR are nearby the CUT.

TABLE I. Targets Description

Angle-Doppler-range cell	SNR (dB)	Angle-Doppler-range cell	SNR (dB)
(0, 0.2, 20)	20	(0.1, 0, 18)	25
(0.2, 0, 20)	20	(-0.1, 0, 18)	25
(0, -0.2, 20)	20	(-0.3, 0.2, 24)	30
(-0.2, 0, 20)	20	(0.3, 0.2, 24)	30
(-0.1 0, 22)	25	(0.3, 0.2, 16)	30
(0.1, 0, 22)	25	(-0.3, 0.2, 16)	30
(0, 0.2, 20)	20	(0.1, 0, 18)	25

A. Air Surveillance Scenario

In this scenario, sequential MF-IAA, sequential APC-IAA, MF-RMVDR, and STRAP employ 10, 10, 5, and 5 adaptive iterations, respectively. For comparison, the result of the conventional training method for estimating clutter covariance matrix is shown in Fig. 1(b). It shows that coherent signals with the same angle are cancelled and it fails to indicate the targets (see [22] for more details). The sequential MF-IAA outputs in Fig. 1(c) is plagued with sidelobes from nearby strong intereference and the sequential APC-IAA in Fig. 1(d) performs much better. In Fig. 1(e), MF-RMVDR is a little better than MF-IAA and worse than APC-IAA in this scenario. Fig. 1(f) shows that STRAP has suppressed nearly all of the space-time-range sidelobes to the level of the noise and demonstrates that it is quite robust against the nearby interference.

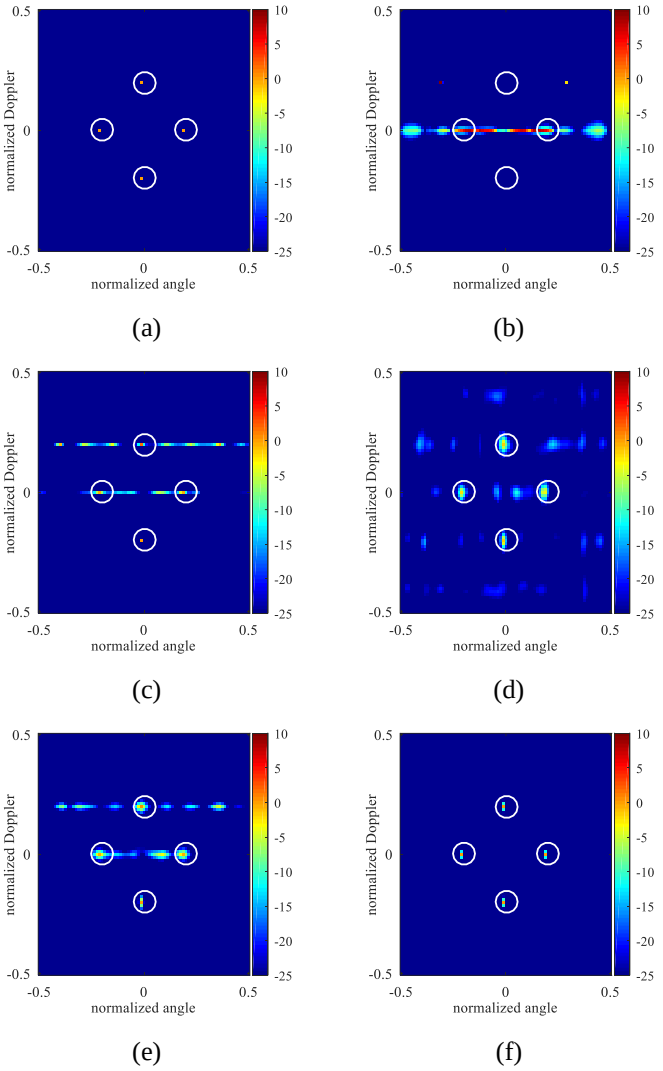

Fig. 1. Angle-Doppler images of (a) true scenario, (b) conventional training method, (c) sequential MF-IAA (d) sequential APC-IAA, (e) MF-RMVDR, (f) STRAP.

B. MTI Scenario

For airborne platform, MIMO radar suffers performance degradation due to the ground clutter. For a side-looking airborne radar with small crab angle, the clutter Doppler frequency depends linearly on the sinusoidal value of the azimuth angle. As shown in Fig. 2(a), the ground clutter in an iso –range ring is distributed along a line, which is called "clutter ridge". In this Scenario, clutter-to-noise ratio (CNR) is fixed at 15 dB and an iso-range ring is divided into 1000 clutter patches. Fig. 2(b) shows that the conventional training method still suffers from coherent signals cancellation. As the clutter is a signal-depended interference, the performance of sequential MF-IAA and sequential APC-IAA in Fig. 2(c), (d) is degraded seriously, however, Fig. 2(e) and (f) show the effectiveness of MF-RMVDR and STRAP, and STRAP outperforms the other methods. This result is a little different from that in the air surveillance scenario and MF-RMVDR shows better performance than sequential APC-IAA. It is because that in the presence of ground clutter, the phase coherence among the

received signals from different pulses and receivers is susceptible to APC, of which the filter weights are different among pulses. Note that in this scenario, sequential MF-IAA, sequential APC-IAA, MF-RMVDR, and STRAP still employ 10, 10, 5, and 5 adaptive iterations, and we find that sequential MF-IAA and sequential APC-IAA keep almost invariant as the number of iterations increases.

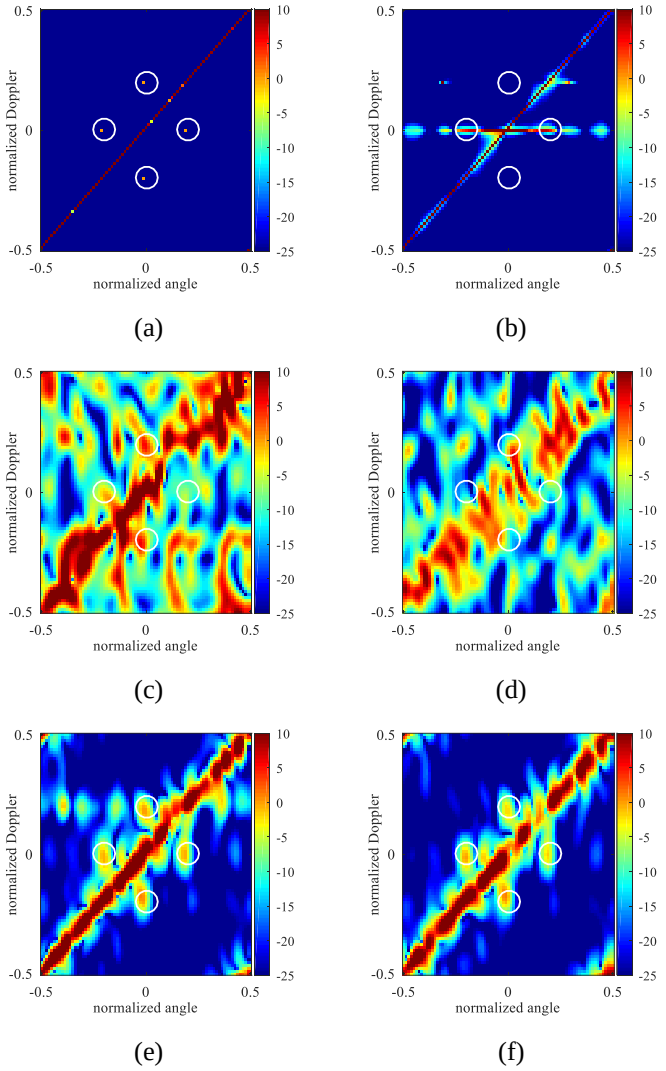

Fig. 2. Angle-Doppler images of (a) true scenario, (b) conventional training method, (c) sequential MF-IAA (d) sequential APC-IAA, (e) MF-RMVDR, (f) STRAP.

VI. CONCLUSIONS

In this paper, a scheme termed STRAP is proposed based on the framework of APC and the criterion of MVDR to overcome the influence of non-completely orthogonal waveforms on MIMO radar imaging. Two specific algorithms are developed and assessed by simulation experiments in air surveillance scenario and MTI scenario respectively. The results show the effectiveness of STRAP. Note that this paper aims to assess the effectiveness of joint space, time and range processing and the huge computational cost is ignored. Nevertheless, further study should be dedicated to the sub-optimal reduced-dimension, reduced-rank or other fast algorithms not well investigated in this paper.

REFERENCES

[1] E. Fishler, A. Haimovich, R. Blum, *et al*, "MIMO radar: an idea whose time has come," in Proceedings of the IEEE Radar Conference, Philadelphia, 2004, pp. 71-78.

[2] E. Fishler, A. Haimovich, R. S. Blum, *et al*, "Spatial diversity in radars-models and detection performance," IEEE Transactions on Signal Processing, vol. 54, pp. 823-838, 2006.

[3] N. H. Lehmann, E. Fishler, A. M. Haimovich, *et al*, "Evaluation of transmit diversity in MIMO-radar direction finding," IEEE Transactions on Signal Processing, vol. 55, pp. 2215-2225, 2007.

[4] J. Li and P. Stoica, MIMO radar signal processing: Wiley-IEEE Press, 2009.

[5] J. Li, L. Xu, P. Stoica, K. W. Forsythe, and D. W. Bliss, "Range compression and waveform optimization for MIMO radar: a cramé-rao bound based study," IEEE Transactions on Signal Processing, vol. 56, pp. 218-232, 2008.

[6] S. D. Blunt and K. Gerlach, "Multistatic adaptive pulse compression," IEEE Transactions on Aerospace and Electronic Systems, vol. 42, pp. 891-903, 2006.

[7] N. Li, J. Tang and Y. N. Peng, "Adaptive pulse compression of MIMO radar based on GSC," Electronics Letters, vol. 44, pp. 1217-2118, 2008.

[8] J. R. Guerci, Space-time adaptive processing for radar, 2rd ed. London, UK: Artech House, 2014.

[9] C. Y. Chen and P. P. Vaidyanathan, "MIMO radar space-time adaptive processing using prolate spheroidal wave functions," IEEE Transactions on Signal Processing, vol. 56, pp. 623-635, 2008.

[10] I. S. Reed, J. D. Mallett and L. E. Brennan, "Rapid convergence rate in adaptive arrays," IEEE Transactions on Aerospace and Electronic Systems, vol. 10, pp. 853-863, 1974.

[11] J. Li, X. Zhu, P. Stoica, and M. Rangaswamy, "High resolution angle-Doppler imaging for MTI radar," IEEE Transactions on Aerospace and Electronic Systems, vol. 46, pp. 1544-1556, 2010.

[12] T. Yardibi, J. Li, P. Stoica, M. Xue, and A. B. Baggeroer, "Source localization and sensing: a nonparametric iterative adaptive approach based on weighted least squares," IEEE Transactions on Aerospace and Electronic Systems, vol. 46, pp. 425-443, 2010.

[13] X. Tan, W. Roberts, J. Li, and P. Stoica, "Range-Doppler imaging via a train of probing pulses," IEEE Transactions on Signal Processing, vol. 57, pp. 1084-1097, 2009.

[14] W. Roberts, P. Stoica, J. Li, T. Yardibi, and F. A. Sadjadi, "Iterative adaptive approaches to MIMO radar imaging," IEEE Journal of Selected Topics in Signal Processing, vol. 4, pp. 5-20, 2010.

[15] T. Higgins, S. D. Blunt and A. K. Shackelford, "Space-range adaptive processing for waveform-diverse radar imaging," in 2010 IEEE Radar Conference, 2010, pp. 321-326.

[16] T. Higgins, S. D. Blunt and A. K. Shackelford, "Time-range adaptive processing for pulse agile radar," in 2010 International Waveform Diversity and Design Conference, 2010, pp. 115-120.

[17] "IEEE standard radar definitions,", 2008, p. 41c1.

[18] F. Gini, A. D. Maio and L. Patton, Waveform design and diversity for advanced radar systems, London, UK: The Institution of Engineering and Technology,2012.

[19] S. D. Blunt and K. Gerlach, "Adaptive pulse compression via MMSE estimation," IEEE Transactions on Aerospace and Electronic Systems, vol. 42, pp. 572-584, 2006.

[20] Z. Li, Y. Zhang, S. Wang, L. Li, and M. Mclinden, "Fast adaptive pulse compression based on matched filter outputs," IEEE Transactions on Aerospace and Electronic Systems, vol. 51, pp. 548-564, 2015.

[21] H. Deng, "Polyphase code design for orthogonal netted radar systems," IEEE Transactions on Signal Processing, vol. 52, 2004.

[22] J. Guan, Y. Huang and Y. He, "A CFAR detector for MIMO array radar based on adaptive pulse compression-Capon fllter," Science China, vol. 54, pp. 2411-2424, 2011